PHYSICAL REVIEW MATERIALS **1**, 052003(R) (2017)

Persistent three- and four-atom orbital molecules in the spinel AlV_2O_4

Alexander J. Browne,[1] Simon A. J. Kimber,[2] and J. Paul Attfield[1,*]

[1]*Centre for Science at Extreme Conditions and School of Chemistry, University of Edinburgh, West Mains Road, Edinburgh EH9 3FD, United Kingdom*

[2]*Chemical and Engineering Materials Division, Oak Ridge National Laboratory, Oak Ridge, Tennessee 37831, USA*

(Received 15 August 2017; published 31 October 2017)

Electronic instabilities in transition-metal compounds may lead to ground states containing orbital molecules when direct metal-metal orbital interactions occur. The spinel AlV_2O_4 was reported to contain V_7^{17+} orbital heptamers that emerge below a 700 K charge ordering transition. Our x-ray total scattering analysis of AlV_2O_4 between 300 and 1100 K reveals a very different picture as the postulated heptamers are found to be pairs of spin-singlet V_3^{9+} trimers and V_4^{8+} tetramers, and these orbital molecules persist to at least 1100 K in a disordered high-temperature cubic phase.

DOI: 10.1103/PhysRevMaterials.1.052003

Notable electronic and magnetic properties arise from the ordering of charge, orbital, and spin degrees of freedom in transition-metal (M) oxides and related compounds [1,2]. When M-M distances are short, for example, through edge or face sharing of MO_6 octahedra, moleculelike clusters of metal cations may be formed if ordering localizes electrons into appropriately oriented d orbitals [3]. Clusters of metal-metal bonded cations formed below an orbital ordering transition have thus been termed "orbital molecules" [4]. A classic exemplar is VO_2, where a metal-insulator transition and accompanying structural (Peierls) distortion at 340 K leads to the formation of $(V^{4+})_2$ dimers within one-dimensional chains from V ions that are uniformly spaced above the transition [5,6]. The importance of moleculelike bonding interactions in driving the dimerization in VO_2, and related materials such as Ti_4O_7, V_4O_7, and NbO_2, has recently been highlighted [7]. More complex arrangements of orbital dimers are found in $CuIr_2S_4$ [8] and $MgTi_2O_4$ [9], and the formation of disordered $(Mo^{4+})_2$ orbital dimers has recently been identified at the spin-glass transition of the pyrochlore $Y_2Mo_2O_7$ [10].

Orbital molecules of more than two M ions are less common. Triangular $(V^{3+})_3$ clusters are found in A_xVO_2 (A = Li,Na) materials and $BaV_{10}O_{15}$ [11–13], while linear Fe_3^{8+} "trimerons" are observed in the complex electronic order of magnetite (Fe_3O_4) below the much-studied Verwey transition [14,15], and coexisting dimers and trimers are reported in the related material Fe_4O_5 [16]. The largest orbital molecules claimed to date are heptameric clusters, reported in AlV_2O_4 below a charge and orbital ordering transition accompanied by a rhombohedral to cubic structural distortion at $T_{CO} = 700$ K [17]. The ground state was reported as having a formal charge distribution $Al_4[V_7^{17+}V^{3+}]O_{16}$, where the V_7^{17+} heptamer has 18 $3d$ electrons occupying nine localized orbitals with an overall spin $S = 0$, while the remaining $S = 1$ V^{3+} cation is paramagnetic. The spin singlet nature of the heptamers was confirmed by ^{51}V NMR measurements [18] and further studies revealed that the long-range charge and orbital ordering is suppressed by replacing V with 5% Cr [19], or by applying pressures over 21 GPa [20].

The conventional picture of orbital molecule formation is that these quantum states emerge by displacive distortions from a structurally uniform high-temperature phase below some electronic and structural transition temperature, ranging from the Peierls transition in VO_2 to an intersecting one-dimensional orbital ordering wave description of the heptamer order in AlV_2O_4 [21]. However, recent studies of local structure through analysis of the pair distribution function (PDF) obtained from total scattering measurements have shown that disordered $4d$ orbital dimers persist above the transition in $LiRh_2O_4$, where $(Rh^{4+})_2$ dimers persist up to 350 K, well above their 170 K ordering temperature [22], and in Li_2RuO_3, where $(Ru^{4+})_2$ dimers order below 540 K but are evident to at least 920 K [23]. However, similar PDF studies of $CuIr_2S_4$ and VO_2 (the only $3d$ transition-metal material investigated in this way) have reported that the orbital dimers disappear from both the long-range and local structure above their transition temperatures [24,25]. To investigate whether large orbital molecules can persist to high temperatures, we have studied the long-range and local structure of AlV_2O_4, and in this Rapid Communication we report a very different picture of the electronic ordering in this material than that previously described.

Polycrystalline AlV_2O_4 was synthesized from powdered Al, V_2O_5, and V_2O_3 ground together in the stoichiometric ratio, pressed into pellets, and sealed in evacuated quartz ampoules for three heatings up to 1150 °C for a total of 96 h, with intermediate regrinding and pelleting. V_2O_3 was prepared by a reduction of V_2O_5 under flowing H_2 at 900 °C. Magnetization measurements shown in the Supplemental Material [30] are similar to those in the literature [17]. High-energy x-ray total scattering data were collected on beamline ID22 at the European Synchrotron Radiation Facility using wavelength $\lambda = 0.206547$ Å. The AlV_2O_4 sample was held in a 0.7-mm-diameter quartz capillary and heated to temperatures between 300 and 1100 K using a hot air blower. Rietveld fits to the x-ray patterns were carried out using the GSAS program [26]. For PDF analysis, background-corrected scattering functions $S(Q)$ were transformed to pair distribution functions $G(r)$, using PDFGETX3 [27], for momentum transfers Q between 0.5 and 25.8 Å^{-1}. Structural models were refined against the PDF data using the PDFGUI program [28], including simulation of termination ripples, over the interatomic distance range $1.5 \leqslant r(\text{Å}) \leqslant 12$. As a further check that orbital molecule features

*j.p.attfield@ed.ac.uk

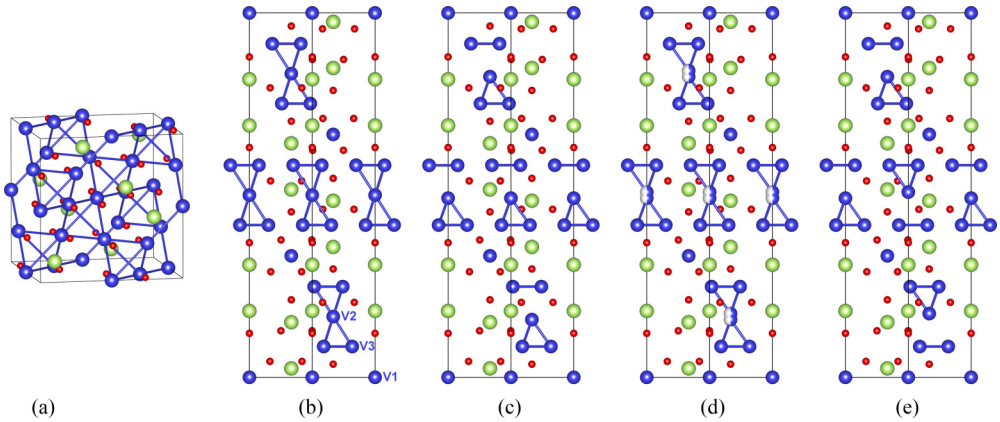

FIG. 1. Structural models for AlV_2O_4 where Al/V/O are green/blue/red atoms. (a) The cubic spinel structure, showing nearest-neighbor V-V connections, which are all equivalent. (b) The previously reported V_7 cluster model with $R\bar{3}m$ symmetry. The three symmetry-independent vanadium sites are labeled: Site V1 is occupied by paramagnetic V^{3+} cations, while each heptamer comprises a central V2 atom between two triangles of V3 atoms. (c) The $R3m$ model used for PDF fitting, in which V_3 and V_4 orbital molecules have long-range ferroelectric order. (d) The split-site $R\bar{3}m$ model used to describe the disordered antiferroelectric average crystal structure in the Rietveld fits. (e) A local configuration showing a statistical distribution of the clusters corresponding to the split-site average in (d). The rhombohedral unit cells in (b)–(e) are projected on the (110) plane with the c axis vertical, and short (<2.90 Å) orbital molecule V-V distances are shown.

extracted from the AlV_2O_4 PDFs are not the result of termination errors or other data artifacts, comparable x-ray data were also collected at 300 K from the cubic spinel LiV_2O_4, which is of interest for heavy fermion behavior [29]. Fits to the LiV_2O_4 PDF do not evidence orbital molecules or other deviations from the cubic spinel structure. These and further structural results for AlV_2O_4 are in the Supplemental Material [30].

AlV_2O_4 is reported to have a cubic spinel structure [Fig. 1(a)] at high temperatures, and a rhombohedral ordered arrangement of V_7 heptamers (space group $R\bar{3}m$) below $T_{CO} = 700$ K [Fig. 1(b)] [17]. However, the $R\bar{3}m$ heptamer model was found to give a poor fit to the PDF derived from 300 K x-ray scattering data, particularly in the 2.4–3.2 Å range where nearest-neighbor V-V distances lie [Fig. 2(a)]. This indicates that the heptamer description of short-range V-V bonding is incorrect. Modifications to the orbital molecule structure were investigated, and a simple change was found to bring the fit into agreement with the PDF in the V-V region. Allowing the central V atom of the heptamers (atom V2 in the structural model) to move in the z direction towards one of the two triangular end faces greatly improves the overall fit [Fig. 2(a)]. This displacement forms separate triangular V_3 and tetrahedral V_4 clusters within which V-V distances are short (<2.7 Å), indicative of bonding, while intercluster V-V distances are much longer (>2.9 Å). Previous measurements indicated that the apparent V_7^{17+} heptamers have a spin singlet ground state [17,18], and the same condition is met by a combination of $S = 0$ V_3^{9+} trimers and $S = 0$ V_4^{8+} tetramers. These result from simple two-center two-electron V-V bonding: Three $3d^2$ V^{3+} ions form two bonds each, giving V_3^{9+} triangles, and four $3d^3$ V^{2+} ions are each bonded to three others in V_4^{8+} tetrahedra. The charge distribution in the ground state of AlV_2O_4 is thus $Al_4[V_4^{8+}V_3^{9+}V^{3+}]O_{16}$, showing an unprecedented coexistence of two large orbital molecules.

The $Al_4[V_4{}^{8+}V_3{}^{9+}V^{3+}]O_{16}$ model was fitted to the low-temperature PDF data by allowing all V2 atoms to displace in the same direction which lowers the space group symmetry to polar $R3m$, although $R\bar{3}m$ symmetry constraints were applied to all other atoms to reduce the number of variables. The long-range ordering of pairs of V_3^{9+} and V_4^{8+} orbital molecules in this $R3m$ model [Fig. 1(c)] is polar and could give rise to ferroelectricity. A simple ordering of antiparallel V2 displacements to give an alternative antiferroelectric order is frustrated in rhombohedral symmetry as the V2 sites are arranged in triangular layers, so the alternative ground state has the disordered structural average shown in Fig. 1(d), where a half-occupied split V2 site models the disorder within each orbital molecule pair. Rietveld fits (shown in the Supplemental Material [30]) of the ferroelectric ordered pair model gave poorer fits than the disordered antiferroelectric average model, hence the latter is taken as our proposed ground-state structure for AlV_2O_4 corresponding to a long-range ordered array of disordered pairs of V_3^{9+} and V_4^{8+} orbital molecules, as shown in Fig. 1(e), equivalent to the split V2 site model of Fig. 1(d) in the crystallographic average.

Above $T_{CO} = 700$ K the structural symmetry of AlV_2O_4 changes from rhombohedral to cubic. The cubic $Fd\bar{3}m$ normal spinel structure [Fig. 1(a)] has one electronically averaged $V^{2.5+}$ site, and all nearest-neighbor V-V distances are equal. However, this model gives a poor fit to the PDF derived from 1100 K x-ray data in the relevant 2.4–3.2 Å region [Fig. 2(b)], suggesting that local V displacements are still present above T_{CO}. To explore whether the V_3^{9+} and V_4^{8+} orbital molecules survive to high temperatures, the $R3m$ model [Fig. 1(c)] was used to fit the PDFs above 700 K. The hexagonal lattice parameters a_H and c_H were constrained to give a metrically cubic lattice ($c_H/a_H = \sqrt{24}$), consistent with the average structure, and all V-V distances within the two orbital molecules were constrained to be equal to improve refinement stability at high temperatures. This model greatly improves the fit to the PDF data [Fig. 2(b)] and the derived V-V distances are found to evolve continuously between the rhombohedral and cubic phases [Fig. 3(a)]. Even at 1100 K, bonding V-V distances within orbital molecules are 2.78 Å and nonbonding

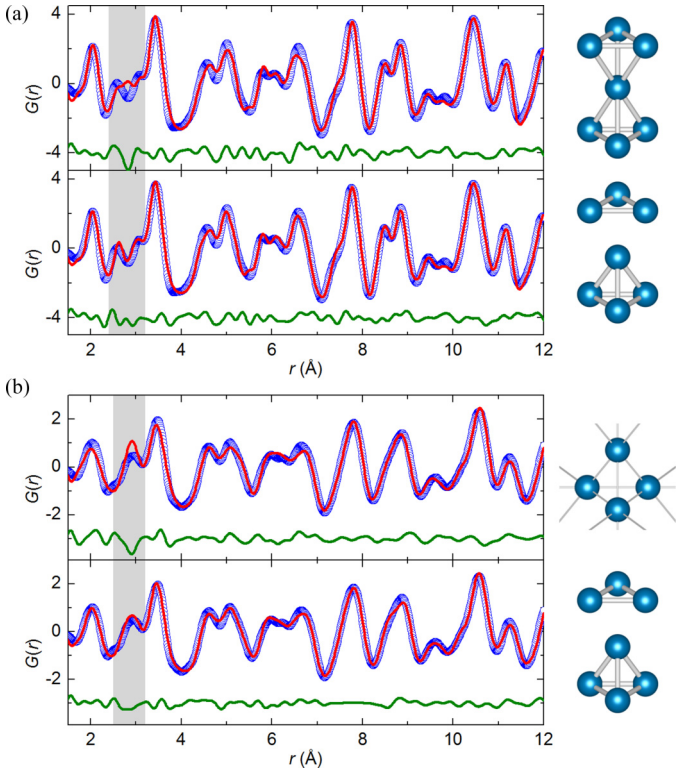

FIG. 2. Comparisons of fits to pair distribution functions (PDFs) of AlV_2O_4 where nearest-neighbor V-V distances lie in the shaded region at $r = 2.4$–3.2 Å. The local vanadium species in each structural model are shown to the right. (a) 300 K PDF, where the upper fit (residual $R_w = 16.3\%$) of the $R\bar{3}m$ V_7 heptamer model [Fig. 1(b)] agrees poorly in the V-V region, but allowing the central V to move off center to form V_3 and V_4 orbital molecules in the $R3m$ model [Fig. 1(c)] gives the improved fit shown below ($R_w = 13.6\%$). (b) 1100 K PDF, where the upper fit of the ideal cubic $Fd\bar{3}m$ spinel model [Fig. 1(a)] gives a poor fit in the shaded region ($R_w = 16.6\%$), but the lower fit of V_3 and V_4 orbital molecules in a $R3m$ model [Fig. 1(c)] constrained by metrically cubic cell parameters greatly improves the agreement ($R_w = 11.6\%$).

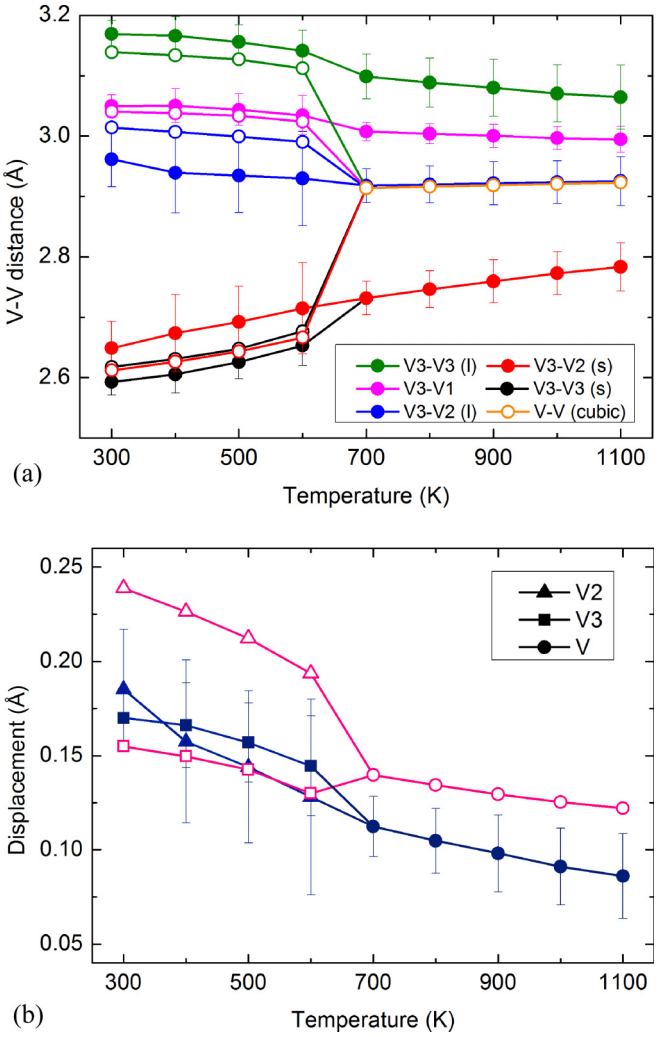

FIG. 3. (a) Comparison of V-V nearest-neighbor distances in AlV_2O_4 from PDF fits (solid symbols) using the $R3m$ structural description, and Rietveld analyses (open symbols) using the split-site $R\bar{3}m$ and cubic $Fd\bar{3}m$ spinel models respectively below and above $T_{CO} = 700$ K. Rietveld V-V distances all converge to a single value above T_{CO} because disordered orbital molecules are not described by a cubic average spinel structure, but PDF fitting shows that they persist above T_{CO}. (The two bonding V-V distances were constrained to be equal in the PDF fits above T_{CO} for refinement stability.) (b) Displacements of V atoms from their ideal sites due to orbital molecule formation, from PDF (solid symbols) and the split-site Rietveld (open symbols) analyses. Both sets of displacements decrease smoothly on heating, but evidence the persistence of orbital molecules to 1100 K.

distances vary between 2.93 and 3.06 Å, whereas the standard cubic spinel description predicts all V-V distances to be 2.92 Å. To describe the disordered orbital molecules within the cubic average structure of $Al_4[V_4^{8+}V_3^{9+}V^{3+}]O_{16}$ in Rietveld fits we used a split-site $Fd\bar{3}m$ model in which 7/8 of the V scattering (representing the proportion of vanadium atoms in orbital molecules) is displaced to two sites either side of the ideal position that holds the remaining 1/8. This leads to an improved fit to all the high-temperature profiles, as shown in the Supplemental Material [30]. Whether the orbital molecules have significant dynamics with motions coupled to the phonon modes at high temperatures is unclear from the present data, and inelastic scattering experiments will be needed to test this possibility.

A comparison of V atom displacements derived from the PDF fits and split-site Rietveld refinements in Fig. 3(b) shows that they agree well, with the V displacement decreasing from ~0.2 Å at 300 K to ~0.1 Å at 1100 K. Extrapolation indicates that zero displacement (i.e., a uniform cubic spinel arrangement) would be reached above ~2000 K, which is far above the ~1400 K synthesis temperature for AlV_2O_4. Previous measurements showed little change in magnetization or conductivity through the transition at $T_{CO} = 700$ K (AlV_2O_4 is a semiconductor with activation energy ~0.4 eV) [31], which corroborates the validity of the $Al_4[V_4^{8+}V_3^{9+}V^{3+}]O_{16}$ description at high temperatures as smaller species derived from the breakdown of the $S = 0$ V_3^{9+} and V_4^{8+} orbital molecules would either lead to large increases in paramagnetic susceptibility from electron-localized states, as the theoretical Curie

constant per V atom changes from $C = 0.125$ emu K mol^{-1} for $Al_4[V_4^{8+}V_3^{9+}V^{3+}]O_{16}$ towards 1.44 emu K mol^{-1} for paramagnetic $AlV^{2+}V^{3+}O_4$, or to increased conductivity through electron delocalization. Hence, AlV_2O_4 has remarkably stable V_3^{9+} and V_4^{8+} orbital molecules that are disordered within the high-temperature cubic spinel phase to at least 1100 K, and form an ordered array of disordered pairs below the apparent charge ordering transition at 700 K.

The structural insights derived from this study demand a substantial revision of theoretical descriptions for the electronic transition in AlV_2O_4 and the physics of large orbital molecule formation. The ground state of AlV_2O_4 is found to contain pairs of spin-singlet V_3^{9+} trimers and V_4^{8+} tetramers, rather than V_7^{17+} heptamers as previously reported. The upper size limit of known orbital molecules is thus reduced from seven- to four-atom clusters. This provides a more consistent size distribution for the known species, with many dimers, a few trimers, and tetrameric V_4^{8+} orbital molecules as the largest example. AlV_2O_4 is thus notable for containing a mixture of the two largest known orbital molecules. The $V_3{}^{9+}/V_4^{8+}$ orbital molecules within each pair in the ground state appear to be disordered, but could lead to a novel ferroelectric state if ordered. High-temperature studies demonstrate that disordered $V_3{}^{9+}$ and V_4^{8+} orbital molecules "hidden" in the crystallographic cubic average structure of AlV_2O_4 persist to at least 1100 K, far above the apparent charge ordering transition at 700 K. The conventional picture of orbital molecules emerging displacively from a structurally uniform phase below the electronic and structural transition is thus incorrect for this spinel. The ideal cubic structure is apparently unstable over all its existence range with respect to local charge and orbital ordering that produces orbital molecules, and their disorder to a pairwise order transition leads to the cubic to rhombohedral structural change observed on cooling below T_{CO}. The temperature scales for the formation and the long-range ordering of orbital molecules are thus very different for AlV_2O_4, unlike in VO_2 in which they are the same [25], showing that orbital molecule phenomena in these apparently similar 3*d*-metal oxides can originate from real-space (molecular) or momentum-space (Fermi surface) electronic instabilities. Reinvestigation of similar materials using local structure methods will thus be important to discover whether "hidden" orbital molecules are present in other apparently uniform average structures.

We thank Mauro Coduri for help with data collection. This work was supported by the ERC and access to ESRF was provided by STFC. Part of this work was supported by the US Department of Energy (DOE), Office of Science, Basic Energy Sciences, at the Oak Ridge National Laboratory.

[1] C. N. R. Rao and B. Raveau, *Transition Metal Oxides* (Wiley-VCH, New York, 1998).
[2] P. A. Cox, *Transition Metal Oxides: An Introduction to Their Electronic Structure and Properties* (Oxford University Press, Oxford, UK, 2010).
[3] J. B. Goodenough, Phys. Rev. **117**, 1442 (1960).
[4] J. P. Attfield, APL Mater. **3**, 041510 (2015).
[5] A. Magnéli, and G. Andersson, Acta Chem. Scand. **9**, 1378 (1955).
[6] F. J. Morin, Phys. Rev. Lett. **3**, 34 (1959).
[7] Z. Hiroi, Prog. Solid State Chem. **43**, 47 (2015).
[8] P. G. Radaelli, Y. Horibe, M. J. Gutmann, H. Ishibashi, C. H. Chen, R. M. Ibberson, Y. Koyama, Y.-S. Hor, V. Kiryukhin, and S. W. Cheong, Nature (London) **416**, 155 (2002).
[9] M. Schmidt, W. Ratcliff II, P. G. Radaelli, K. Refson, N. M. Harrison, and S. W. Cheong, Phys. Rev. Lett. **92**, 056402 (2004).
[10] P. M. M. Thygesen, J. A. M. Paddison, R. Zhang, K. A. Beyer, K. W. Chapman, H. Y. Playford, M. G. Tucker, D. A. Keen, M. A. Hayward, and A. L. Goodwin, Phys. Rev. Lett. **118**, 067201 (2017).
[11] T. Jin-no, Y. Shimizu, M. Itoh, S. Niitaka, and H. Takagi, Phys. Rev. B **87**, 075135 (2013).
[12] M. Guignard, D. Carlier, C. Didier, M. R. Suchomel, E. Elkaïm, P. Bordet, R. Decourt, J. Darriet, and C. Delmas, Chem. Mater. **26**, 1538 (2014).
[13] T. Kajita, T. Kanzaki, T. Suzuki, J. E. Kim, K. Kato, M. Takata, and T. Katsufuji, Phys. Rev. B **81**, 060405(R) (2010).
[14] E. J. W. Verwey, Nature (London) **144**, 327 (1939).
[15] M. S. Senn, J. P. Wright, and J. P. Attfield, Nature (London) **481**, 173 (2012).
[16] S. V. Ovsyannikov *et al.*, Nat. Chem. **8**, 501 (2016).
[17] Y. Horibe, M. Shingu, K. Kurushima, H. Ishibashi, N. Ikeda, K. Kato, Y. Motome, N. Furukawa, S. Mori, and T. Katsufuji, Phys. Rev. Lett. **96**, 086406 (2006).
[18] Y. Shimizu, M. Tanaka, M. Itoh, and T. Katsufuji, Phys. Rev. B **78**, 144423 (2008).
[19] K. Matsuno, T. Katsufuji, S. Mori, M. Nohara, A. Machida, Y. Moritomo, K. Kato, E. Nishibori, M. Takata, M. Sakata, K. Kitazawa, and H. Takagi, Phys. Rev. Lett. **90**, 096404 (2003).
[20] S. Kalavathi, S. Vennila Raju, S. Chandra, Q. Williams, and P. Ch. Sahu, Solid State Commun. **250**, 23 (2017).
[21] M. Croft, V. Kiryukhin, Y. Horibe, and S.-W. Cheong, New J. Phys. **9**, 86 (2007).
[22] K. R. Knox, A. M. M. Abeykoon, H. Zheng, W.-G. Yin, A. M. Tsvelik, J. F. Mitchell, S. J. L. Billinge, and E. S. Bozin, Phys. Rev. B **88**, 174114 (2013).
[23] S. A. J. Kimber, I. I. Mazin, J. Shen, H. O. Jeschke, S. V. Streltsov, D. N. Argyriou, R. Valentí, and D. I. Khomskii, Phys. Rev. B **89**, 081408(R) (2014).
[24] E. S. Božin, A. S. Masadeh, Y. S. Hor, J. F. Mitchell, and S. J. L. Billinge, Phys. Rev. Lett. **106**, 045501 (2011).
[25] S. A. Corr, D. P. Shoemaker, B. C. Melot, and R. Seshadri, Phys. Rev. Lett. **105**, 056404 (2010).
[26] A. C. Larson and R. B. Von Dreele, General Structure Analysis System (GSAS), Los Alamos National Laboratory Report No. LAUR 86-748, 2004 (unpublished).
[27] P. Juhás, T. Davis, C. L. Farrow, and S. J. L. Billinge, J. Appl. Crystallogr. **46**, 560 (2013).

[28] C. L. Farrow, P. Juhas, J. W. Liu, D. Bryndin, E. S. Božin, J. Bloch, Th. Proffen, and S. J. L. Billinge, J. Phys.: Condens. Matter **19**, 335219 (2007).

[29] S. Kondo *et al.*, Phys. Rev. Lett. **78**, 3729 (1997).

[30] See Supplemental Material at http://link.aps.org/supplemental/10.1103/PhysRevMaterials.1.052003 for further details of magnetic susceptibility, PDF, and Rietveld analyses. Open data for this article are at http://datashare.is.ed.ac.uk/handle/10283/838.

[31] K. Matsuno, T. Katsufuji, S. Mori, Y. Moritomo, A. Machida, E. Nishibori, M. Takata, M. Sakata, N. Yamamoto, and H. Takagi, J. Phys. Soc. Jpn. **70**, 1456 (2001).